



Kinetic and mechanical properties of dual curable adhesives for display bonding process



Jong-Gyu Lee^a, Gyu-Seong Shim^a, Ji-Won Park^a, Hyun-Joong Kim^{a,*}, Kwan-Young Han^b

^a *Laboratory of Adhesion and Bio-Composites, Program in Environmental Materials Science, Seoul National University, Seoul, 151-921 Republic of Korea*

^b *Display Engineering, College of Convergence Technology, Dankook University, 330-714 Republic of Korea*

ARTICLE INFO

Article history:

Accepted 1 July 2016

Available online 9 July 2016

Keywords:

Dual curable adhesive

Dual curing behavior

Optically clear resin

Crosslinking

Adhesion performance

ABSTRACT

UV–thermal dual curable adhesives were prepared using an acrylic resin with 2,2′-azobis(4-methoxy-2,4-dimethyl valeronitrile), which exhibits ten hour half-life decomposition temperature of 30 °C, in order to address issues related to monomers that cannot be cured in a shaded area during the display bonding process. We investigated the dual curing behavior of the resin with variations in the UV dose and in the thermal radical initiator content, and we also assessed the influence of the dual curing on the mechanical properties. The curing behavior was assessed through the use of photo-DSC and FT-IR conversion. In addition, the degree of crosslinking was investigated via gel fraction, and the thermal properties were measured via DSC and TGA. Peel strength, probe tack and pull-off tests were performed to evaluate the bonding performance of the dual curable adhesives. The adequate level of thermal radical initiator (TRI) content to obtain a high conversion and degree of crosslinking was approximately 0.1 phr. These were the optimum values to adjust the balance between the unstable state and the insufficient contents, and the thermal curing behavior was promoted with an increase in the UV dose and in the thermal initiator content. The gel fraction and the FT-IR ATR results clearly indicate that an enhanced network structure was formed under low UV and high thermal radical initiator content conditions. Therefore, in a low UV dose condition, the mechanical properties improved, even with a low molecular weight due to a high network formation.

© 2016 Elsevier Ltd. All rights reserved.

1. Introduction

The display bonding process involves coalescing the window and touch screen panel (TSP) of a device using PSAs or transparent adhesives, such as optically clear resin (OCR) or optically clear adhesive (OCA) [1,2]. The reason to apply OCR or OCA on the entire surface of the display is to adhere the TSP and the window and to protect the TSP from an external impact. In addition, this also reduces the loss of light since it minimizes the reflection of light by filling up the air gap between the glass and the panel [3]. The window is divided into two parts: a transparent part of the display and a black matrix (BM) through which light cannot pass. UV light cannot penetrate under the BM area, and so unreacted monomer can cause reliability issues and pollution near the circuit board. The process to simply use light to cure the adhesive is therefore limited in that it cannot be used to cure the shaded area. A side that is overshadowed by the flexible printed circuit board (FPCB)

does not achieve fully cure, even if the device goes through a side curing process that irradiates light in different directions.

Industry has been increasingly using UV curing because doing so has various advantages including a fast curing speed, low energy consumption, processability at room temperature, low VOCs emissions, etc. [4,5]. In addition, the UV curing process is being considered to replace traditional solvent-borne processes because it is more ecologically friendly and has excellent properties. In particular, acrylate is widely used for the UV radical polymerization because it has a high reactivity [6]. However, the use of a UV curing process has a major disadvantage in that the shaded areas where light cannot reach cannot be cured [7]. For example, the curved portion of an automobile coating and the BM area for a display bonding process cannot be completely cured by only using a UV curing process [8,9]. This insufficient conversion can result in the elution of materials and can limit the mechanical properties of the polymer due to its low molecular weight [10–12].

As a result, various studies have been carried out on dual curing materials that not only respond to a UV curing process but also incorporate other methods of curing. Park et al. [13] described the

* Corresponding author. Tel.: +82 2 880 4784; mobile: +82 10 7123 4784.

E-mail address: hjokim@snu.ac.kr (H.-J. Kim).

dual curing mechanism for epoxy acrylate by forming crosslinking between the hydroxyl group and epoxy group. Studer et al. [14] observed the network formation of an acrylic copolymer containing isocyanate and a hydroxyl group in the branch during thermal curing. Hwang et al. [9] studied dual curing behavior and rheology using a thermal radical initiator for automotive applications. Shan et al. [15] explored the application of a UV–thermal dual curing system for electrically conductive adhesives (ECAs).

In this study, 2,2'-azobis(4-methoxy-2,4-dimethyl valeronitrile), which decays by 1st order chemical kinetics and has 30 °C of ten hour half-life decomposition temperature, was used with an acrylic prepolymer, photo radical initiator and a crosslinking agent. An initiator with a low decomposition temperature was used because the touch screen panel could be damaged at a high temperature during thermal curing, and it was also used to make it possible to cure the material with the ambient temperature of the metal halide UV lamp chamber. A minimum amount of initiator was added because the resin becomes unstable as excessive thermal radical initiator (TRI) is added, and other problems may occur, such as self-curing, undissolving and yellowing during storage. In previous studies, adding more than 0.2 phr of the initiators resulted in an unstable state [16]. On the other hand, a photo radical initiator was added in a sufficient amount to cure the shaded area during side curing with a low UV dose and to reduce the process time as much as possible. During the process, the dual curing behavior was measured in a UV dose of 0, 400, 800 and 1600 mJ/cm² because curing can proceed in a variety of pre-UV curing conditions due to the randomness of UV penetration. Table 1 provides the sample names of each of the dual cured adhesives. Isobornyl acrylate, 2-ethylhexyl acrylate, and N-vinyl caprolactam were used as monomer. Poly(ethylene glycol (200) dimethacrylate) was used as a crosslinking agent. Fig. 1 shows the brief procedure to prepare the sample. Then, FT-IR was used to investigate the chemical reactions within the adhesive. The formation of a cross-linked structure was evaluated through a gel fraction. The curing behavior was also evaluated via DSC and TGA, and peel strength, probe tack and pull-off tests were conducted to assess bond strength.

Table 1
Formulations and operating conditions for dual curable adhesives.

Name	UV dose (mJ/cm ²)	TRI contents (phr)
DCA-0000	0	0
DCA-0002		0.02
DCA-0005		0.05
DCA-0010		0.1
DCA-0400	400	0
DCA-0402		0.02
DCA-0405		0.05
DCA-0410		0.1
DCA-0800	800	0
DCA-0802		0.02
DCA-0805		0.05
DCA-0810		0.1
DCA-1600	1600	0
DCA-1602		0.02
DCA-1605		0.05
DCA-1610		0.1

2. Experimental

2.1. Materials

2-Ethylhexyl acrylate (2-EHA, Sigma Aldrich, USA), isobornyl acrylate (IBA, Sigma Aldrich, USA) and N-vinyl caprolactam (VC, Tokyo Chemical Industry, Japan) were used as monomers. Poly(ethylene glycol (200) dimethacrylate) (PEGDMA 200, Miwon Specialty Chemical, Republic of Korea) was used as a difunctional monomer to produce the network structure in the adhesives. Hydroxydimethyl acetophenone (Micure HP-8, Miwon Specialty Chemical, Republic of Korea) was used as a photo radical initiator. 2,2'-Azobis(4-methoxy-2,4-dimethyl valeronitrile) (V-70, Wako Pure Chemical Industries, Japan) was used as the thermal radical initiator. All reagents were used without any further purification. The chemical structures of each monomer and initiator are shown in Fig. 2.

2.2. Characterization methods

2.2.1. Prepolymer synthesis

The prepolymer was prepared using 2-EHA (61%), IBA (35%) and VC (4%) via bulk radical polymerization under UV irradiation with 1 wt% of photo radical initiator. Polymerization was performed in a 500 ml four-necked rounded-bottomed flask equipped with a mechanical stirrer, N₂ inlet, thermometer and LED UV lamp with wavelength of 365 nm. The temperature was maintained at room temperature with constant stirring with 100 rpm. After purging with N₂ for 30 min with constant stirring, the monomer mixtures were exposed to a UV lamp (20 mW/cm²) for 70 s under N₂ purging [17].

2.2.2. Preparation of adhesive film

The dual curable adhesives were prepared by blending prepolymer with 1 phr of crosslinking agent and thermal radical initiator. The mixture was mixed with a paste mixer at 600 rpm and 500 rpm for 3 min. The acrylic resin was coated to a 100-μm thickness on corona-treated polyethylene terephthalate films (PET, SKC Co. LTD., Republic of Korea). The coated resin was cured by UV curing using a UV conveyor equipped with medium pressure mercury UV-lamps with an intensity of 154 mW/cm² and main wavelength of 365 nm. The irradiated UV doses were of 200, 400, 800 and 1600 mJ/cm². The UV doses were measured using a UV radiometer (IL 390 C Light Bug, International Light Inc.). Each of the pre-cured adhesives with various curing degrees was cured in an oven at 80 °C for 5, 10 and 30 min.

2.2.3. Fourier transform infrared spectroscopy (FT-IR)

The IR spectra of the samples were observed using Fourier-transform infrared spectrometry (JASCO FTIR-6100) equipped with an attenuated total reflectance (ATR) accessory. The spectra were collected with 32 scans at a resolution of 4 cm⁻¹ between 4000 and 400 cm⁻¹. The acrylate double bond conversion was calculated using Eq. (1)

$$\text{Conversion(\%)} = \frac{(A_{810})_0 / (A_{1720})_0 - (A_{810}) / (A_{1720})}{(A_{810})_0 / (A_{1720})_0} \times 100 \quad (1)$$

where (A₈₁₀)₀ is the intensity for 810 cm⁻¹ at the initial time and (A₈₁₀) is the intensity for 810 cm⁻¹ after curing [18].

2.2.4. Gel fraction

The gel fraction of the dual curable adhesives after UV curing and thermal curing was determined by soaking the samples in toluene for 1 day at room temperature. The amounts of the sample were about 5 g. In addition, the insoluble part of the adhesives was filtered with a 40 mesh net and dried at 70 °C.

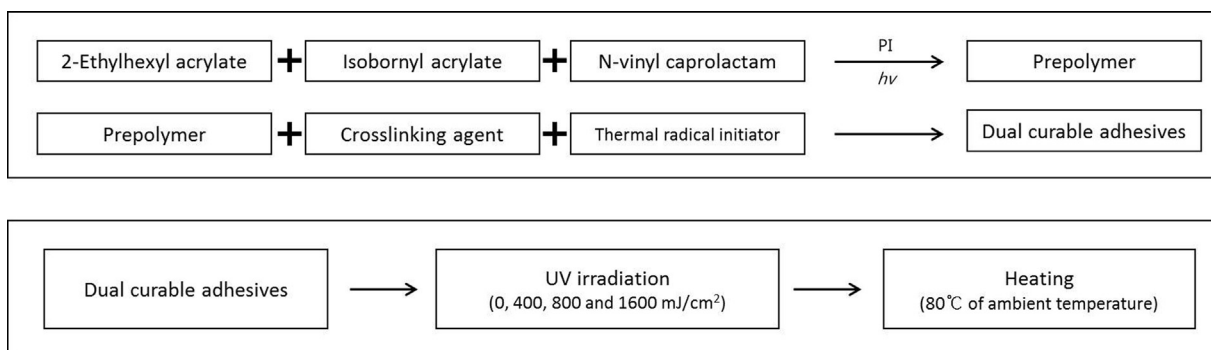


Fig. 1. Preparation and curing process for dual curable adhesives.

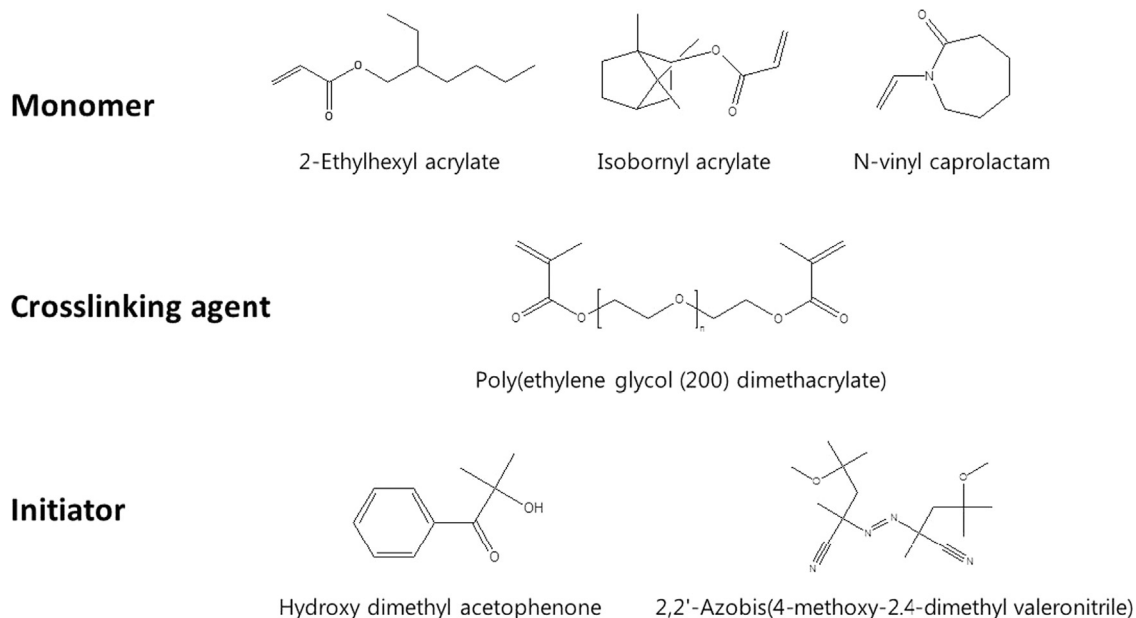


Fig. 2. Chemical structures of the various compounds used in this study.

2.2.5. Thermogravimetric analysis (TGA)

TGA measurements were carried out using a thermogravimetric analyzer (TGA 4000, Perkin Elmer, USA). The samples of 7–10 mg were evaluated from 50 to 400 °C at a heating rate of 5 °C/min. During the test, the dual cured adhesives and the resin were placed in an inert nitrogen atmosphere (99.5% nitrogen, 0.5% oxygen content) to prevent unwanted oxidation.

2.2.6. Differential scanning calorimetry (DSC)

Differential scanning calorimetry (DSC) measurements were carried out using a TA Q200 differential scanning calorimeter with a scanning temperature ranging from –50 to 200 °C at a scanning rate of 2 °C/min with an isothermal test at 80 °C for 30 min. The analysis was carried out with samples of 7–8 mg each. Each sample was scanned in the dynamic mode and was cooled at the same rate under a nitrogen atmosphere. The thermal curing behavior was determined from the first scan. The glass transition temperature (T_g) was determined during the second scan.

2.2.7. Photo-differential scanning calorimetry (photo-DSC)

Photo-DSC measurements were taken using a TA Q200 differential scanning calorimeter equipped with a UV irradiation accessory (Omniscure 2000) that used UV light from a 100 W middle-pressure mercury lamp with a range in wavelength from 300 to 400 nm. The UV light level of the UV accessory with a 90% UV filter was 10. The analysis was carried out for samples of 1.5–

2 mg in an open aluminum DSC pan. After UV irradiation, the thermal curing behavior was determined with a scanning temperature range from 30 to 80 °C at a scanning rate of 2 °C/min.

2.2.8. Adhesion performance

2.2.8.1. Peel adhesion. The adhesive films that were prepared were attached to a stainless steel substrate, and a 2 kg rubber roller was passed over them twice. The specimens for the peel strength test were made with width of 25 mm. The 180° peel strength was measured using a Texture Analyzer (TA-XT2i, Micro Stable Systems, UK) after the sample had been left to stand at room temperature for 24 hours. The peeling speed was 300 mm/min, and the average strength of the peeling period was measured 5 times.

2.2.8.2. Probe tack. A debonding speed of 0.5 mm/s was maintained on the surface of the adhesives for 1 s under a constant force of 100 g/cm², and the probe tack was measured as the maximum debonding force. The tack measurements of the adhesive films were carried out with a TA-XT2i Texture Analyzer (Micro Stable Systems, UK) at 25 °C using a probe tack consisting of a polished stainless steel (type 304) cylinder probe with a diameter of 5 mm.

2.2.8.3. Pull-off test. On the glass surface, the dual-curable adhesives were loaded and crosswise covered with a glass slide (75 × 25 × 1 mm³), as portrayed in Fig. 3. These assemblies were

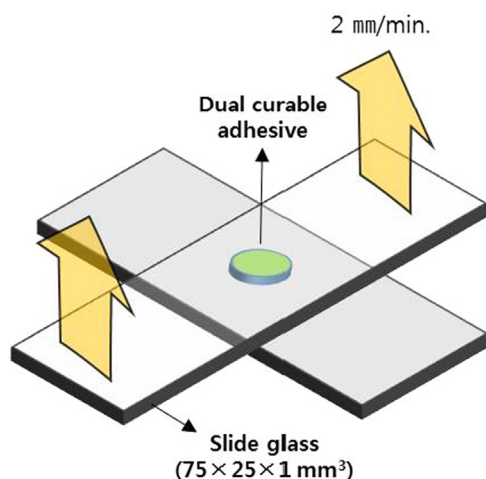


Fig. 3. Schematic diagram of the assembly for the measurement of pull-off test.

cured using UV-curing equipment with a 100-W high-pressure mercury lamp (Main wavelength of 340 nm). The UV dose was of 0, 400, 800 and 1600 mJ/cm². The UV doses were measured with an IL 390 C Light Bug UV radiometer (International Light, Inc., USA). Next, the UV-cured assemblies were cured in a drying oven for 30 min at 80 °C. Measurements of adhesion strength were performed at room temperature with a crosshead speed of 2 mm/min.

3. Results & discussion

3.1. Curing behavior of acrylic resin determined by DSC

DSC and photo-DSC are a form of thermal analysis that provides the curing kinetics of the polymerization of the dual curable adhesives. The polymerization of the acrylic resin is achieved through the destruction of the C=C bond, and the reaction of the monomer and the kinetics are analyzed by measuring the heat flow [19,20]. It is not easy to evaluate the UV-curing behavior because the UV-curing process is very fast. In this respect, photo-DSC is an adequate evaluation method that can be used to analyze the UV curing behavior. The reactivity of the acrylic resin is assessed by plotting the heat flow against time and temperature in order to describe the UV curing and thermal curing behavior.

Fig. 4a–c shows the UV curing behavior and the thermal curing behavior after UV irradiation as the initiator content was changed. In Fig. 4a and b, the UV curing behavior is evaluated through UV irradiation each for 0, 6, 60 s through the use of a metal halide lamp in photo-DSC. As shown in Table 2, the integration area was 0.85 J/g for 6 s, and the area was 4.4 J/g for 60 s. The 6-s curing time was set to have a 20% curing level for the 60 s cure time. Even when the content of the thermal initiator increases, the UV curing behavior is not affected, so no change is found for the peak time and the exothermic area. Fig. 5 shows the thermal curing behavior of the residual monomer through a temperature scan after UV irradiation. When the initiator content increased from 0.02 phr to 0.1 phr, the reactivity for the thermal curing became accelerated. This can be found on the graph where the starting temperature increases 10.4 °C with 0 s of UV irradiation and increases 9.5 °C with 6 s of irradiation. In addition, the exothermic peak of the thermal curing decreases as the UV irradiation increases for the 0.1 phr TRI contents, but the same amount of 68 J/g were released for both the 0 s and 6 s UV irradiation conditions with 0.02 phr of TRI content. This is because the amount of reaction for the 0.1 phr

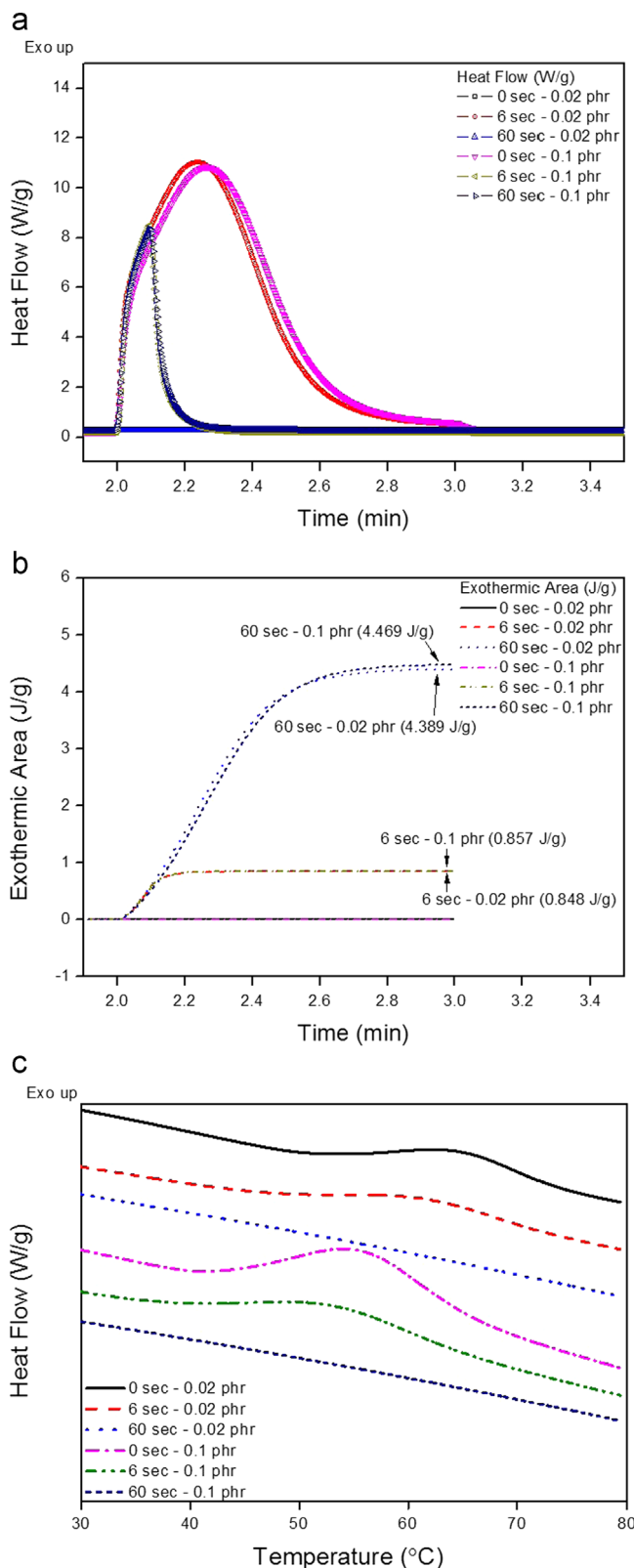


Fig. 4. (a) Heat flow and (b) exothermic area of UV curing behavior and (c) thermal curing behavior of the dual curable adhesives according to the different UV dose and TRI contents.

of TRI decreased by exhausting the monomers as the UV curing progressed. However, a sufficient amount of remaining monomer can be cured without a reduction in the reactivity at 0.02 phr of TRI.

Table 2
Peak heat flow, peak temperature and exothermic area by photo-DSC.

UV curing time (s)	Initiator contents (phr)	UV curing		Thermal curing		
		Maximum heat flow (W/g)	Exothermic area (J/g)	Starting temperature (°C)	Peak temperature (°C)	Exothermic area (J/g)
0	0.02	–	–	52.5	64.5	68.1
	0.1	–	–	42.1	55.6	195.9
6	0.02	8.49	0.85	46.6	61.4	68.6
	0.1	8.36	0.86	37.1	53.3	125.1
60	0.02	11.02	4.39	–	–	–
	0.1	10.85	4.47	–	–	–

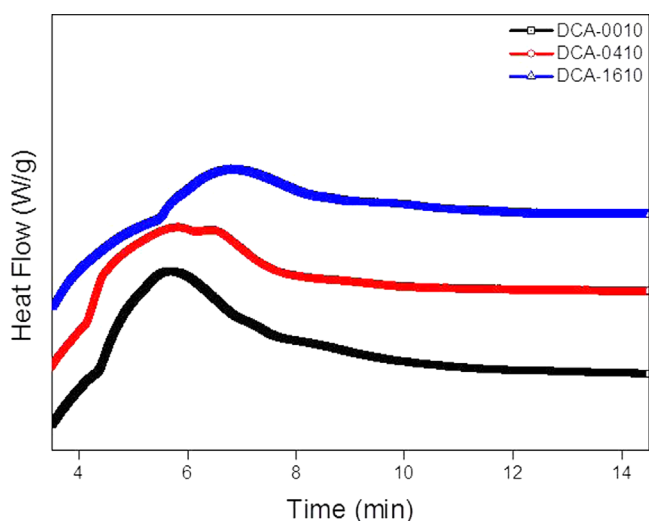


Fig. 5. Thermal curing behavior at 80 °C isothermal condition with different pre-UV dose condition.

In Fig. 5, the adhesive films (DCA-0010, DCA-0410 and DCA-1610) that were irradiated by 0, 400 and 1600 mJ/cm² of UV doses in a UV conveyor show a curing behavior at 80 °C in isothermal conditions. When the curing behavior of the three adhesive films was checked, the peak height decreased as the UV dose increased in the following order: DCA-0010, DCA-0410 and DCA-1610. A comparison of the samples without UV irradiation shows that the thermal curing peak rapidly forms with DCA-0410, but the reactivity rather decreases with DCA-1610. Therefore, the photo-DSC and DSC results indicate that UV curing rarely is affected even if TRI is being added, and when TRI content increases, the reaction peak shifts to a lower temperature. In addition, thermal curing suppression is not affected with a small amount of UV irradiation, but the thermal curing is suppressed when UV curing sufficiently progresses.

3.2. FT-IR conversion

The change in the chemical bond during polymerization of the acrylic resin was evaluated via FT-IR ATR spectroscopy. The amount of reaction can be measured via FT-IR because the C=C bond of the acrylic resin was consumed during polymerization. Fig. 6a shows the FT-IR spectra after UV irradiation of the acrylic resin at 0, 400, 800 and 1600 mJ/cm² irradiation. The 1410 cm⁻¹ peak of vinyl C-H in the plane bend and 810 cm⁻¹ peak of the C=C bond were reduced depending on the UV curing progress. In addition, the 1680 cm⁻¹ peak for amide decreased, and the peak of the secondary C-N amine increased. The change in the

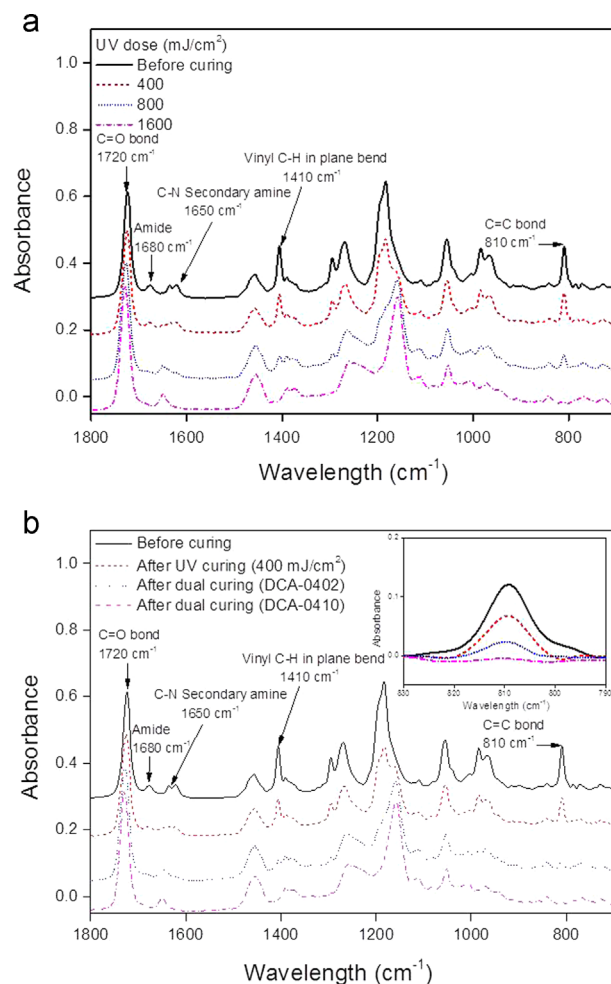


Fig. 6. FT-IR spectra of dual cured adhesives with different UV dose and TRI contents before and after (a) UV curing and (b) dual curing.

amine peak was caused by a reaction of the N-vinyl caprolactam. This result confirms that the lactam ring of N-vinyl caprolactam opened as the reaction proceeded and was converted to secondary amine. Eq. (1) can be used to calculate the conversion as 25% at 400 mJ/cm², 70% at 800 mJ/cm² and 99% at 1600 mJ/cm².

Fig. 6b shows the change in the FT-IR spectra during the dual curing process after irradiation with 400 mJ/cm² of UV light. A comparison of the peaks of DCA-0402 with DCA-0410 indicates that DCA-0402 had a higher absorbance peak at a wavelength of 810 cm⁻¹ because the small amount of initiator was not enough for the reaction to produce enough radicals. In addition, the amide

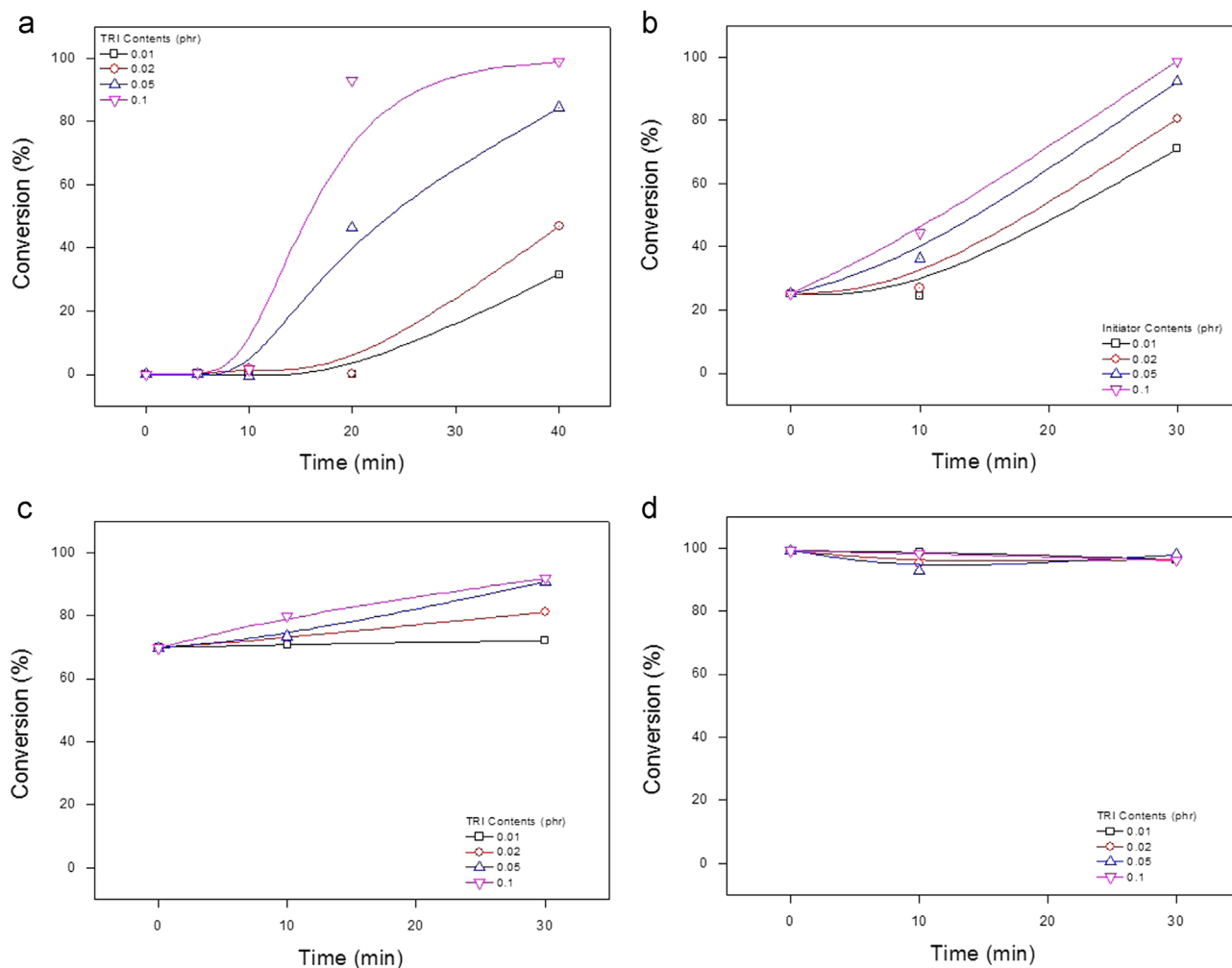


Fig. 7. FT-IR conversion of dual cured adhesives with TRI contents (a) without UV dose, and with UV doses of (b) 400 mJ/cm², (c) 800 mJ/cm² and (d) 1600 mJ/cm².

peak decreased, the secondary amine peak increased, and the chemical changes were observed to be similar to those of adhesives cured only with UV light even though dual curing was performed with a low UV dose.

As shown in Fig. 7, the conversion was used to evaluate the curing behavior with various UV doses during the UV–thermal dual curing process. When the UV dose increased, the reactivity of the thermal curing was accelerated, but the dual curable adhesives with TRI content of less than 0.1 phr cannot generate sufficient radicals to ensure sufficient conversion. Fig. 7a shows the change in conversion with a different initiator content with the 0 mJ/cm² samples. For the 10 min curing time, the conversion did not change for all initiator contents. As previously mentioned, the conversion at a 30 min curing time indicates insufficient conversion when using a low initiator content. However, Figs. 7b and 8c show that thermal curing was observed at 10 min, which indicates that thermal curing accelerated, as shown in Fig. 4. However, Fig. 7d shows the change in the conversion that rarely occurred due to the exhausted C=C bond resulting from UV irradiation at 1600 mJ/cm².

3.3. Gel fraction

The degree of crosslinking can be obtained by measuring the gel fraction through the use of the network polymer that is not soluble in any solvent. PEGDMA 200 can be added to the acrylic resin to form crosslinking. Fig. 8 shows the change in the degree of

crosslinking as a function of both UV dose and initiator content. Here, the degree of crosslinking does not exceed approximately 80% because 20% of linear polymer was formed when the pre-polymer was prepared. Fig. 8a indicates the extent of crosslink formation for 0 mJ/cm². In a manner similar to that in Fig. 7a, crosslinking did not form when heating was employed for 10 min. Fig. 8b–d indicates the change in the gel fraction for the 400, 800 and 1600 mJ/cm² UV doses. The gel fraction gradually decreases, which is different from what is shown in Fig. 7. In addition, the network structure formed with UV curing until 70% of the monomer had been polymerized, as shown in the similar gel fractions at 800 mJ/cm² and at 1600 mJ/cm² for the 0 min heating time, as compared to that shown in Fig. 7c and d. However, for the 800 mJ/cm² UV irradiation condition, the gel fraction increased after heating due to the residual monomers contributing to the formation of the crosslinking as dual curing had proceeded through.

3.4. Thermal analysis of dual curable adhesives determined by DSC and TGA

Fig. 9 shows the DSC curves of the dual curable adhesives that were used to evaluate the change in the glass transition temperature (T_g) in response to changes in the concentration of the initiator and in the UV dose. DCA-0400 did not exhibit a T_g in the samples exposed to a UV dose of 400 mJ/cm², and it was -38.1 °C for DCA-0402 and -35.4 °C for DCA-0410. DCA-1600, DCA-1602

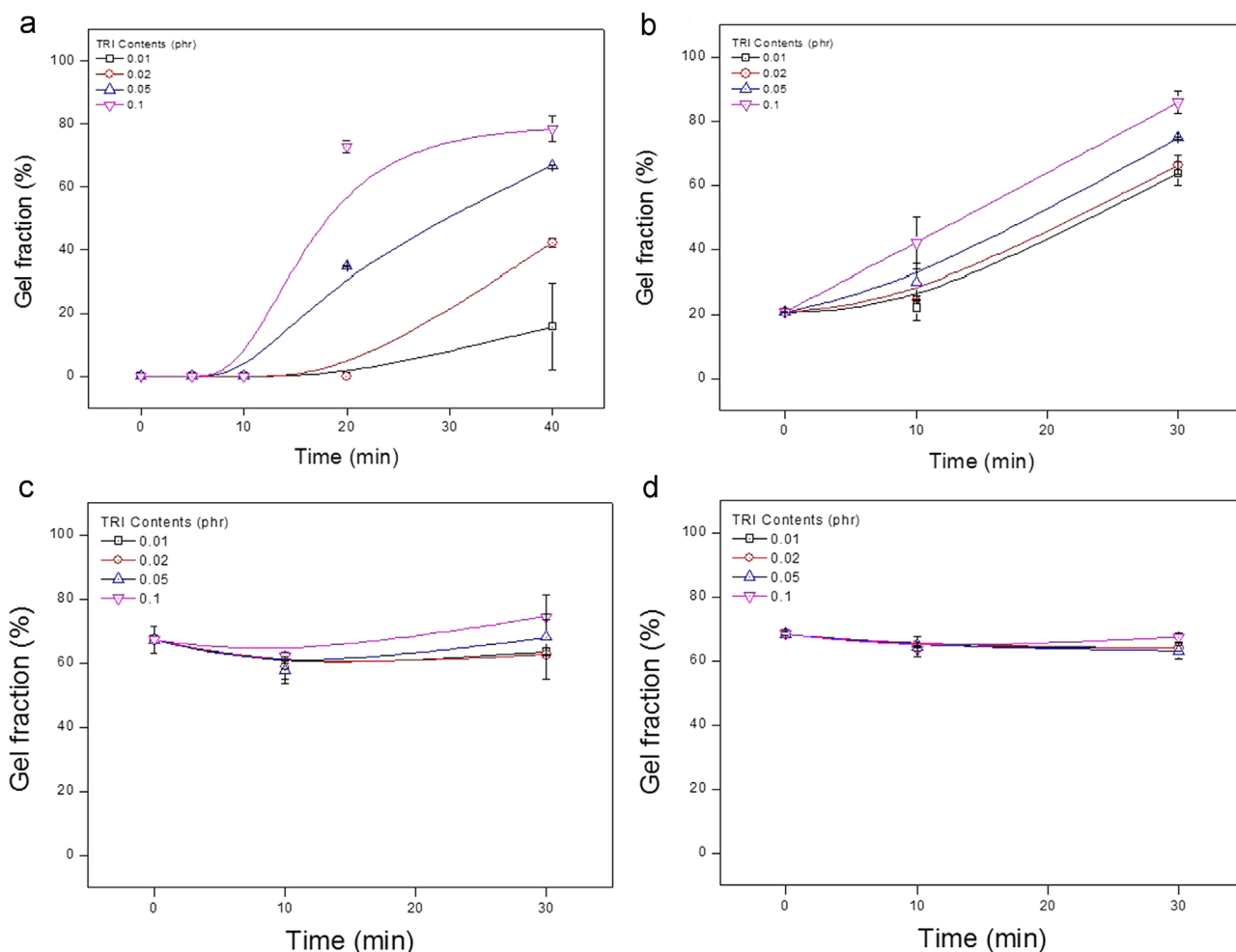


Fig. 8. Gel fraction of dual cured adhesives with TRI contents (a) without UV dose, and with UV doses of (b) 400 mJ/cm², (c) 800 mJ/cm² and (d) 1600 mJ/cm².

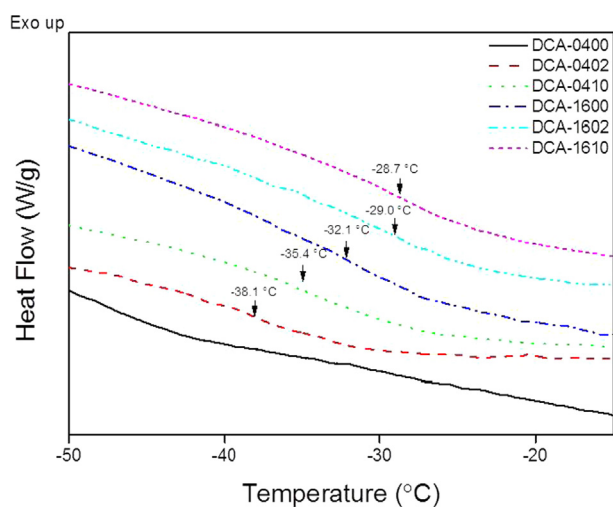


Fig. 9. Glass transition temperature of dual cured adhesives measured by DSC after dual curing.

and DCA-1610 received a UV dose of 1600 mJ/cm², and exhibited a T_g of -32.1 °C, -29.0 °C and -28.7 °C respectively. The change in T_g indicates a change in the structure of the polymer because the copolymer of the resin has the same monomer composition. The increase in T_g with an increase in initiator content is mainly affected by the conversion, as shown in Fig. 7. Since this process does not fully cure the samples with low initiator content, a low T_g

is exhibited due to the formation of a low molecular weight polymer and the remaining residual monomers. In the curing condition with 1600 mJ/cm² of UV irradiation, a higher T_g was exhibited than for DCA-0410 due to the increase resulting from the formation of a higher molecular weight polymer. The 20% conversion at 400 mJ/cm² of UV irradiation will have a lower molecular weight than when continuing the propagation due to UV curing because this is terminated during the propagation reaction. Therefore, even though it has a higher degree of crosslinking, as shown in Fig. 8, T_g is exhibited for the high temperature. Thermal curing after 1600 mJ/cm² of UV irradiation increases T_g due to a decrease in the segmental mobility of the polymer. However, it was not significantly affected by the TRI content because a small amount of TRI can sufficiently react with the remaining monomers.

TG and DTG curves are shown in Fig. 10a and b, which allow an assessment of the composition of the polymers and their thermal stability [21,22]. The thermal stability of the network polymer is affected by the structure of the polymer, composition, flexibility, etc. [23]. The degradation in the dual curable adhesive can be divided into two steps. A weight loss occurs from 50 to 180 °C and degradation is apparent from 270 to 350 °C. The tendency for degradation was observed to be similar for all of the dual curable adhesives because of their similar composition. The first step of the degradation between 50 and 180 °C resulted from the volatilization of unreacted monomer and moisture in the adhesive film. As listed in Table 3, the TGA curves of the dual curable adhesives irradiated with UV at 400 mJ/cm² showed that the sample without

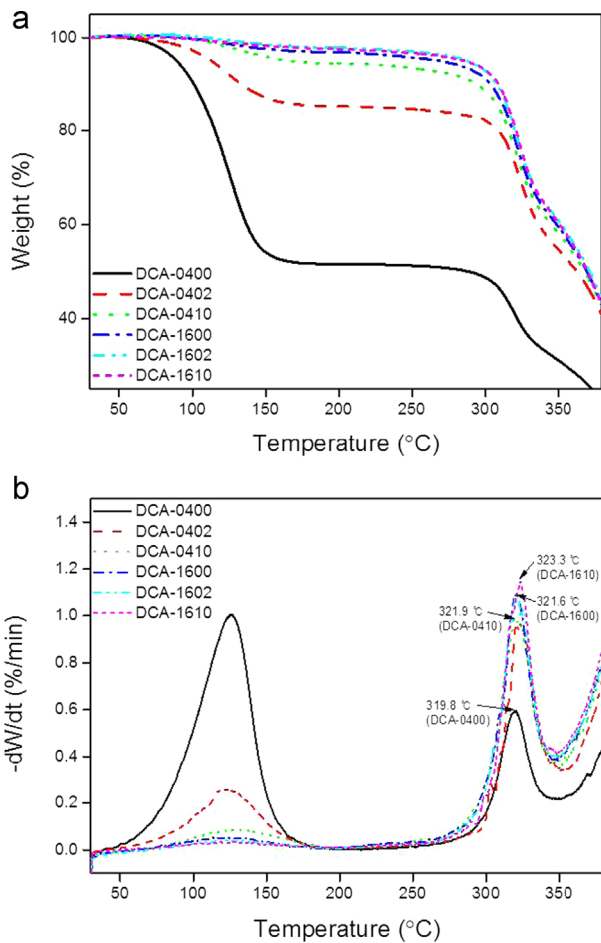


Fig. 10. (a) TG and (b) DTG curves of dual cured adhesives.

Table 3
(a) Thermal decomposition and (b) peak temperature of DTG curves.

Samples	First step		Second step	
	Weight loss @ 200 °C (%)	Peak temperature (°C)	Weight loss @ 350 °C (%)	Peak temperature (°C)
DCA-0400	48.4	125.8	68.9	319.8
DCA-0410	5.5	129.4	42.0	321.9
DCA-1600	3.1	125.9	40.5	321.6
DCA-1610	2.5	126.3	39.6	323.3

added TRI exhibited a 48.4% weight loss between 50 and 200 °C, and the degradation decreased by 14.6% and 5.5% with an increase in the initiator to 0.02 phr and 0.1 phr of TRI content respectively. However, the dual cured adhesives irradiated with 1600 mJ/cm² of UV light did not exhibit a significant weight loss due to the virtual elimination of monomer, due to polymerization, under this irradiation condition. The DTG curves show a slight increase in the thermal resistance during the second step of degradation, in a manner similar to *T_g* with an increase in Fig. 9, as the TRI content and the UV irradiation increased, which is due to the decrease in the chain mobility resulting from the reaction of the remaining monomer.

3.5. Adhesion performance measured by peel strength, probe tack and pull-off test

The peel strength is a common indicator of the adhesion and bond performance of pressure sensitive adhesives, and the probe

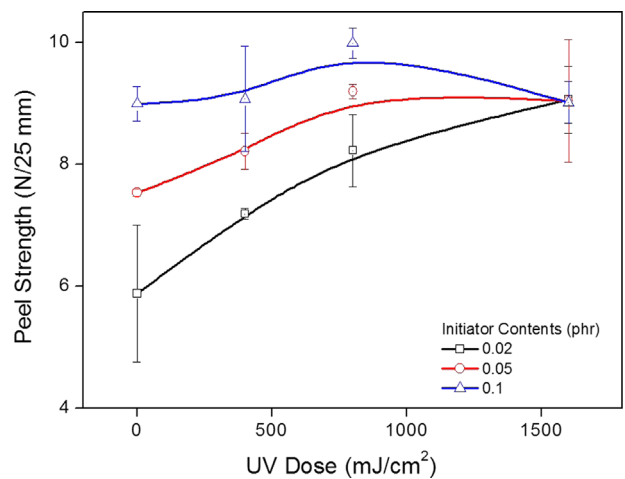


Fig. 11. Peel strength of dual cured adhesives according to the different UV dose and TRI contents.

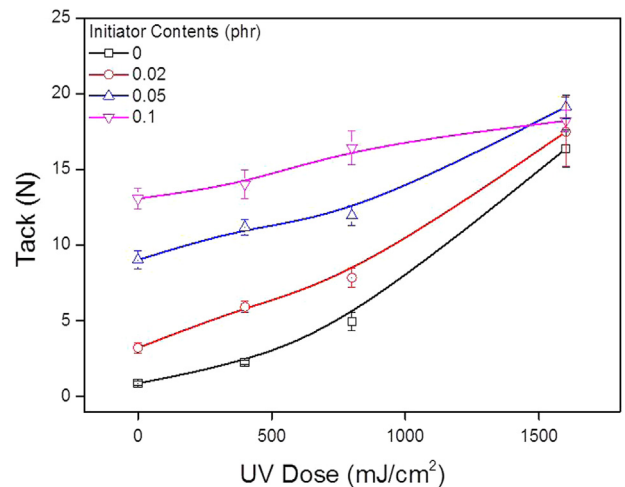


Fig. 12. Probe tack of dual cured adhesives according to the different UV dose and TRI contents.

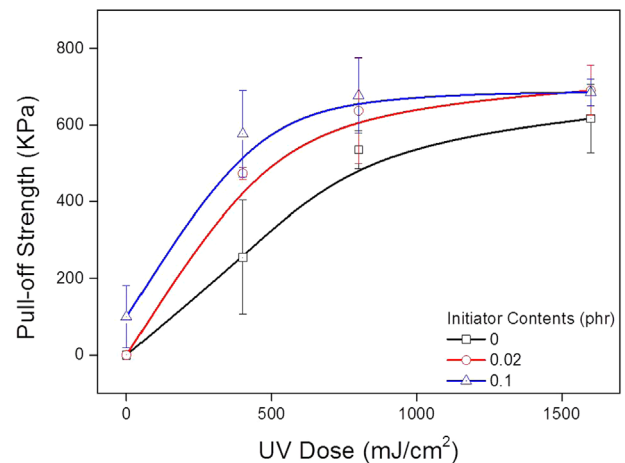


Fig. 13. Pull-off strength of dual cured adhesives according to the different UV dose and TRI contents.

tack indicates the adhesive force over a short time. The pull-off test is an important measurement for application in the display bonding process. The results of the dual curing process with

different initiator contents and UV doses were assessed with respect to the peel strength, probe tack and pull-off test. Fig. 11 shows 180° peel strength values as a function of both initiator concentration and UV irradiation dose together with assessments of the extent of interfacial failure with all the systems examined. As indicated peel strength increases with an increase in conversion as the initiator content increases. However, the dual cured adhesive with a 800 mJ/cm² UV dose has a higher peel strength than that with a 1600 mJ/cm² dose because dual cured adhesives with a lower UV dose had a higher degree of crosslinking [24]. In the case

with 1600 mJ/cm², the peel strength was not affected when the majority of the monomers had reacted during the UV curing process.

As shown in Fig. 12, tack increased as the UV dose increased at all TRI concentrations. The tack of the adhesive containing 0.1 phr of TRI increased due to the linear or branched chain ends that do not form a network structure, in contrast to the tendency shown for peel strength [25]. Dual cured adhesives with different TRI contents were affected by the increase in conversion. As shown in Fig. 13, pull-off strength increases with an increase in both UV dose and TRI content. This is influenced by the mobility of the polymer more than by the impact of the degree of crosslinking. In Fig. 14a–c, the s–s curves of the dual curable adhesives are shown. As initiator was added in the samples with 400 mJ/cm² UV dose, the force and elongation increased due to the increase in conversion. At 800 mJ/cm², the elongation and pull-off strength increased due to the formation of a semi-interpenetrating network (semi-IPN) structure with a linear polymer generated due to UV curing. However, in the 1600 mJ/cm² UV dose, the DCA-16 series shows similar adhesion strength and Young's modulus in the s–s curve due to the formation of a high molecular weight linear polymer, with thermal curing having little impact. However, elongation decreased along with the molecular mobility of the polymer because temporary physical bonding was formed by thermally curing the remaining monomers.

3.6. Network formation of dual curable adhesives

So far we have analyzed the curing behavior, crosslinking formation, thermal properties and adhesion performance of the dual curable adhesives. Fig. 15 shows plots of the data used to analyze the molecular formation of the adhesive cured via dual curing. The conversion represents the consumption of the C=C bond, the gel fraction for the formation of crosslinking, and the results at 200 °C from the TG tests suggest that remaining monomer and moisture had been removed. The conversion in Fig. 15 is different from that shown in the data in Fig. 8, which evaluated curing behavior in the state resin to compare the status of the monomer at 810 cm⁻¹ in order to predict the overall molecular formation. The conversion and TG weight increase in a similar manner. However, the gel fraction increases steeply with the DCA-04 series and shows almost no change in the DCA-16 series. The dual cured adhesives with 400 mJ/cm² of UV irradiation exhibited a gel fraction that increased by only 20% with a 28.8% increase in conversion. Similarly, the gel fraction increased more sharply than conversion for DCA-0400 and DCA-1600. The gel fraction increased by 47.7% as the conversion increased by 55.6%. However, the dual cured adhesives cured with heat show a higher gel fraction than conversion.

Fig. 16 shows the network formation processes of dual curable adhesives with 400 mJ/cm² and 1600 mJ/cm² of UV dose. For UV

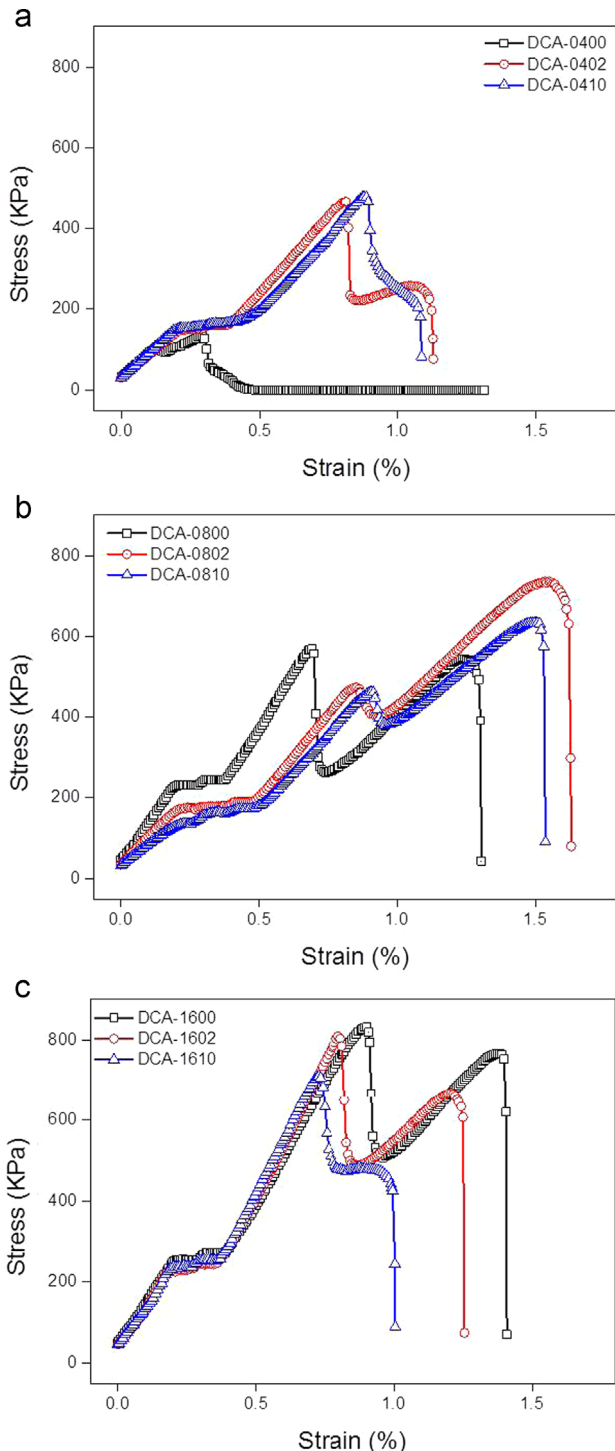


Fig. 14. Stress–strain curves of pull-off test of dual cured adhesives with UV dose of (a) 400 mJ/cm², (b) 800 mJ/cm² and (c) 1600 mJ/cm².

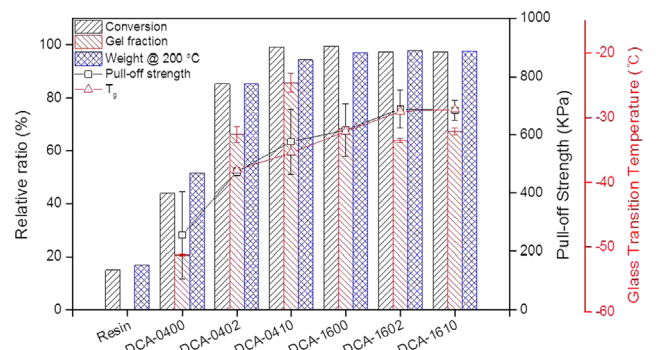


Fig. 15. Correlation between the network formation and the other properties.

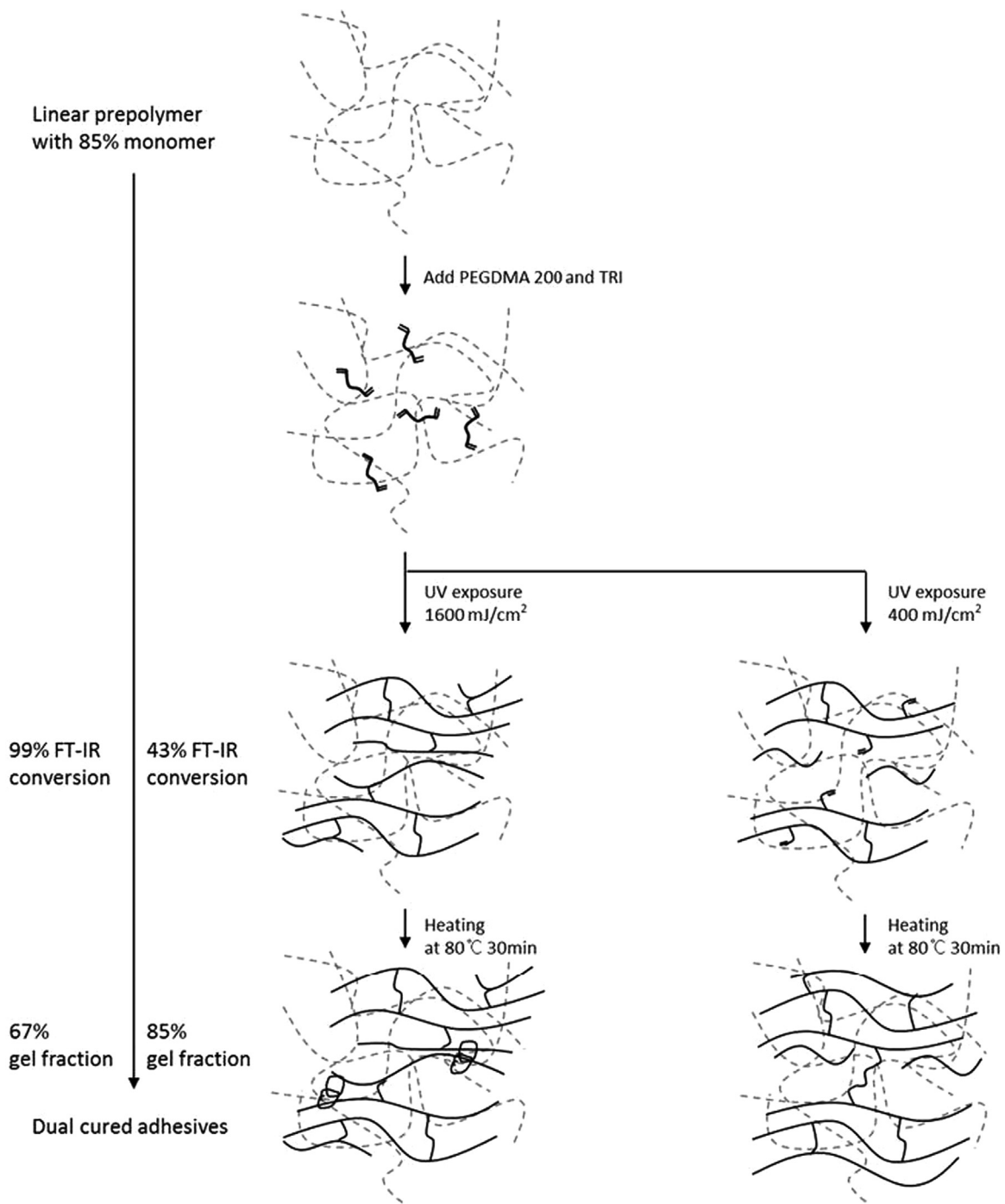


Fig. 16. Schematic diagram of network formation of dual curable adhesives.

curing, the reaction terminates within 1 min because the reaction rate is very fast at room temperature. In addition, since UV curing has a high initiator content, linear polymer formation and network formation happened at the same time. In the case of the formation of the network polymer only with a multifunctional monomer, the volume relaxation was observed to have been delayed as UV curing progressed, and a high degree of crosslinking was obtained [26]. However, this explanation is not adequate for the case of the semi-IPN, which contains a low level of multifunctional monomer. In the conditions with a high level of UV irradiation, the formation of the network structure was limited because the molecular bulk mobility was restricted, and the diffusion-limited termination mechanism was dominant [27]. However, thermal curing occurred

at a higher temperature than UV curing, and the free volume increased. In addition, the lower TRI content than photo-initiator affected the network formation. As a result, the dual curing process provides higher network formation because the step-by-step UV–thermal curing prevents autoacceleration and mobility for the polymer. Therefore, the network is formed by linking the branch of crosslinking agent of each with the molecule to increase segmental mobility, and these characteristics can be observed in terms of the mechanical properties. For the 1600 mJ/cm² UV dose, a strong force was caused by the increase in branched chain ends, and these even had a high molecular weight. Furthermore, the pull-off strength increases in proportion to T_g . When the initiator is added, a small amount of monomer remaining in the dual cured

adhesives reacts to form a temporary physical crosslink that increases T_g due to the decrease in the molecular mobility.

4. Conclusions

Our goal was to investigate the curing behavior and mechanical properties of dual curable adhesives using both UV and thermal radical polymerization. A dual curable system was introduced for the display bonding process to achieve curing under the shaded area. The UV curing behavior of the UV–thermal dual curing was not hindered by the addition of TRI. On the contrary, a higher pre-UV curing and TRI content improved the thermal curing rate. We showed that the application of a dual curing system using UV–thermal radical polymerization is useful for the display bonding process due to the requirement of a low reaction temperature and a short amount of time with good adhesion performance. Relative to pure acrylic adhesives, dual curable adhesives exhibited a higher conversion rate and improved mechanical properties. Our results show that the pre-cured sample with a low UV dose formed a network structure as a result of the low initiator content and higher temperature condition that affected the formation of the gel by linking the crosslinking agent inside the chain. Despite the low molecular weight, which can adversely affect mechanical properties, dual curable adhesives with a low UV dose had similar mechanical properties as those that received a high UV dose because they could be complemented by the network formation. In addition, the initiator content considerably affects curing and molecular forming. The 0.1 phr TRI content formulation was suitable for the dual curable system because a higher TRI content caused bubbles and yellowing, and a lower TRI content could not sufficiently cure the resin. In conclusion, the dual curable adhesives exhibit excellent adhesion for both high and low UV doses when combined with an appropriate initiator content.

References

- [1] Jang ES. Recent development in silicone liquid optically clear adhesive (LOCA) for high and large vehicle display touch screen applications; 2012. p. 69–71.
- [2] Daniel L. Liquid optically clear adhesive for display applications. In: Proceeding of Display Week 2012 Exhibitors' Form; 2012.
- [3] Chang EP, Holguin Daniel. Curable optically clear pressure-sensitive adhesives. *J Adhes* 2005;81:495–508.
- [4] Decker C, Nguyen TV, Decker D, Weber-Koehl E. UV-radiation curing of acrylate/epoxide systems. *Polymer* 2001;42:5531–41.
- [5] Davison S. Technology and applications of UV and EB curing. London: SITA: Technology Limited, Exploring the Science; 1999.
- [6] Andrzejwska E. Photopolymerization kinetics of multifunctional monomers. *Prog Polym Sci* 2001;26:605–65.
- [7] Shmid U. Proceedings of RadTech Europe conference; 2001. p. 53.
- [8] Park S, Hwang JW, Kim KN, Lee GS, Nam JH, Noh SM, et al. Rheology and curing characteristics of dual-curable clearcoats with hydroxyl functionalized urethane methacrylate oligomer: effect of blocked isocyanate thermal crosslinkers. *Korea-Aust Rheol J* 2014;26:159–67.
- [9] Hwang JW, Kim KN, Lee GS, Nam JH, Noh SM, Jung HW. Rheology and curing characteristics of dual-curable automotive clearcoats using thermal radical initiator derived from O-imino-isourea and photo-initiator. *Progress Org Coat* 2013;76:1666–73.
- [10] Witzel MF, Calheiros FC, Goncalves F, Kawano Y, Braga RR. Influence of photoactivation method on conversion, mechanical properties, degradation in ethanol and contraction stress of resin-based materials. *J Dent* 2005;33:773–9.
- [11] Eliades T, Eliades G, Brantley WA, Johnston WM. Residual monomer leaching from chemically cured and visible light-cured orthodontic adhesives. *Am J Orthod Dentofac Orthop* 1995;108:316–21.
- [12] Kim MJ, Kim KH, Kim YK, Kwon TY. Degree of conversion of two dual-cured resin cements light-irradiated through zirconia ceramic disks. *J Adv Prosthodont* 2013;5:464–70.
- [13] Park Y-J, Lim D-H, Kim H-J, Park D-S, Sung I-K. UV- and thermal-curing behaviors of dual-curable adhesives based on epoxy acrylate oligomers. *Int J Adhes Adhes* 2009;29:710–7.
- [14] Studer K, Decker C, Beck E, Schwalm R. Thermal and photochemical curing of isocyanate and acrylate functionalized oligomers. *Eur Polym J* 2005;41:157–67.
- [15] Shang Q, Hao S, Zhang J, Gong J, Wang F, Wu Y, et al. Investigation on constitution of electrical conductive adhesives fitting for UV–thermal dual curing. *J Adhes Sci Technol* 2015;29:910–23.
- [16] Studer K, Nguyen PT, Decker C, Beck E, Schwalm R. Redox and photoinitiated crosslinking polymerization. *Progress Org Coat* 2005;54:230–9.
- [17] Kim S, Lee S-W, Lim D-H, Park J-W, Park C-H, Kim H-J. Fabrication of optically clear acrylic pressure-sensitive adhesive by photo-polymerization: UV-curing behavior, adhesion performance, and optical properties. *J Adhes Sci Technol* 2013;27:2177–90.
- [18] Joo HS, Park YJ, Do HS, Kim HJ, Song SY, Choi KY. The curing performance of UV-curable semi-interpenetrating polymer network structured acrylic pressure-sensitive adhesives. *J Adhes Sci Technol* 2007;21:575–88.
- [19] Boey F, Rath SK, Ng AK, Abadie MJM. Cationic UV cure kinetics for multifunctional epoxies. *J Appl Polym Sci* 2002;86:518–25.
- [20] Nelson EW, Jacobs JL, Scranton AB, Anseth KS. Photo-differential scanning calorimetry studies of cationic polymerizations of divinyl ethers. *Polymer* 1995;36:4651–6.
- [21] Trovati G, Sanches EA, Neto SC, Mascarenhas YP, Chierice GO. Characterization of polyurethane resins by FTIR, TGA, and XRD. *J Appl Polym Sci* 2010;115:263–8.
- [22] Bruce Prime R. Thermal characterisation of polymeric materials. New York: Academic Press; 1981.
- [23] Chattopadhyay DK, Panda SS, Raju KVS. Thermal and mechanical properties of epoxy acrylate/methacrylates UV cured coatings. *Progress Org Coat* 2005;54:10–9.
- [24] Bae K-Y, Lim D-H, Park J-W, Kim H-J, Jeong H-M, Takemura A. Adhesion performance and surface characteristics of low surface energy psas fluorinated by UV polymerization. *Polym Eng Sci* 2013;53:1968–78.
- [25] Czech Z. Synthesis and cross-linking of acrylic PSA systems. *J Adhes Sci Technol* 2007;21:625–35.
- [26] Bowman CN, Peppas NA. Coupling of kinetics and volume relaxation during polymerizations of multiacrylates and multimethacrylates. *Macromolecules* 1991;24:1914–20.
- [27] Anseth KS, Decker C, Bowman CN. Real-time infrared characterization of reaction-diffusion during multifunctional monomer polymerizations. *Macromolecules* 1995;28:4040–3.